

Photophysics and Photochemistry of Diphenyl Sulfone. 2. Investigation of the S_1 Decay Pathways

Maria Cristina Bruni, Glauco Pontzerini,* and Marco Scoponi

Dipartimento di Chimica, Università di Modena, via Campi 183, 41100 Modena, Italy
(Received: November 19, 1987; In Final Form: June 30, 1988)

An extensive analysis of the S_1 deactivation pathways of diphenyl sulfone (DPS) in alcohols and some other solvents is presented. The combined results of steady-state photolysis, time-resolved fluorescence, and steady-state fluorescence measurements at variable temperature and of $S_1 \rightsquigarrow T_1$ intersystem crossing quantum yield determinations enable a complete characterization of the S_1 photophysics and photochemistry of DPS to be obtained. The main S_1 decay channel appears to be an activated $S_1 \rightsquigarrow T_n$ intersystem crossing ($E_a \cong 2$ kcal/mol), other than $S_1 \rightsquigarrow T_1$. Although the fluorescence emission and $S_1 \rightsquigarrow T_1$ quantum yields show some solvent dependence, they play minor roles in the solvents studied. The state eventually reached in the $S_1 \rightsquigarrow T_n$ activated intersystem crossing is proposed to be a dissociative $^3\sigma\sigma^*$ state localized on a C-S bond, on the basis of experimental evidence and of some preliminary theoretical data. A simple rationalization of the observations is provided by a model potential energy diagram obtained as an extension of the one previously proposed to account for the results concerning the T_1 decay of the same molecule. Two hypotheses on the mechanisms of the above-mentioned $S_1 \rightsquigarrow T_n$ activated intersystem crossing are put forward and briefly discussed.

Introduction

An extensive investigation of the singlet and triplet photochemical behaviors of diphenyl sulfone (DPS) has been undertaken recently in our laboratory. The results concerning the lowest triplet state were presented in a previous paper.¹ They clearly demonstrated the existence of a spin-allowed T_1 decay path leading to a C-S homolytic cleavage. A potential energy surface model, characterized by an avoided crossing between the lowest $^3\pi\pi^*$ state and a $^3\sigma\sigma^*$ dissociative state along the stretching coordinate of a C-S bond, was shown to account for the experimental observations. A parallel investigation on *p,p'*-diaminodiphenyl sulfone (ADPS) suggested that the same model could be extended to the T_1 decay of this molecule.

The possibility that the S_1 state of DPS contributes to the C-S bond photocleavage was already suggested in ref 1, on the basis of qualitative laser flash photolysis observations. In this paper, we present the results of an experimental investigation of the S_1 state decay of DPS. Steady-state photolysis, measurement of the fluorescence parameters and of the $S_1 \rightsquigarrow T_1$ intersystem crossing quantum yields, and analysis of the temperature dependence of the fluorescence lifetime provide pieces of information which, when put together, offer a consistent quantitative picture of the S_1 decay pathways of DPS in alcohols and confirm the existence of an important singlet contribution to the molecular photodegradation. Comparison with the S_1 behavior in some different solvents is made. A simple extension of the model proposed in ref 1 for the T_1 decay is shown to rationalize all the new observations and measurements. No quantitative analysis of the S_1 decay of DPS has been previously reported in the literature. The only conclusion of a luminescence study of DPS and some *p,p'*-disubstituted derivatives² is that fluorescence emission is a minor decay pathway of the S_1 states of all the investigated compounds. A second minimum (besides the spectroscopic one), corresponding to a twisted intramolecular charge-transfer (TICT) state, has been shown to exist on the S_1 surface of two *p,p'*-dianilino sulfones in polar solvents.³ However, such a minimum is unlikely to occur in the absence of some electron-donating group opposite to $-\text{SO}_2-$, such as *p*- NH_2 . Indeed, the spectral and kinetic data reported in this paper show that it does not need to be invoked to account for the fluorescence properties of DPS in alcohols.

Results and Discussion

1. Nature of the S_1 State. The lowest energy absorption band of DPS in ethanol and the corrected fluorescence spectra in ethanol and cyclohexane are shown in Figure 1. The shape and position of the absorption band in cyclohexane were the same as in ethanol. This band has been related to the benzenic 1L_b band after comparison of the benzene, methylphenyl sulfone, and DPS absorption spectra.⁵ Such an assignment has been confirmed by a recent CS-INDO/CI calculation⁶ which showed this band to be caused by the transition to one of the two nearly degenerate states describable in terms of exciton coupling of the two benzenic 1L_b transitions. The radiative transition to the other 1L_b -type state is forbidden if a C_{2v} symmetry is assumed for DPS (an assumption in qualitative agreement with both experimental⁷ and theoretical⁶ conformational studies).

The fluorescence spectrum in cyclohexane features a rather blurred structure that resembles the more pronounced structure of the corresponding absorption band and a modest Stokes shift. (The distance between the maxima of the fluorescence and absorption spectra is ~ 2750 cm^{-1} .) This suggests that the ground and S_1 state minima are roughly superimposed. Passage to ethanol only causes weak effects, such as an increased blurring of the vibrational structure and a small red shift (~ 400 cm^{-1}) of the emission band. No double emission is observable in this solvent, a fact which suggests that TICT formation does not occur in the DPS S_1 state.

2. Photodissociation Products and Effect of a Triplet Quencher on the Rate of Product Formation. Irradiation with a low-pressure mercury lamp causes the absorption spectra of DPS in alcohols to undergo rapid changes. Figure 2 shows the time evolution of the absorption spectrum of an irradiated ethanol solution of DPS. The same behavior was observed in methanol. Among the many products contained in the photolyzed ethanol solution, our analysis, based on UV absorption and fluorescence spectroscopy, enabled us to identify benzene and benzenesulfonic acid. The presence of phenol and 1-phenylethanol was also strongly suspected. Some evidence was finally obtained for the formation of 4-biphenyl phenyl sulfone (Ph-Ph-SO₂-Ph), the phenyl ester of benzenethiosulfonic acid (Ph-SO₂-S-Ph), and diphenyl disulfide (Ph-S-S-Ph), which are responsible for the absorption growth at λ

(1) Pontzerini, G.; Momicchioli, F. *J. Phys. Chem.* **1988**, *92*, 4084.

(2) Abdul-Rasoul, F.; Catherall, C. L. R.; Hargreaves, J. S.; Mellor, J. M.; Phillips, D. *Eur. Polym. J.* **1977**, *13*, 1019.

(3) Rettig, W.; Chandross, E. A. *J. Am. Chem. Soc.* **1985**, *107*, 5617.

(4) Leandri, G.; Mangini, A.; Passerini, R. *Gazz. Chim. Ital.* **1954**, *84*, 73.

(5) Jaffè, H. H.; Orchin, M. *Theory and Application of Ultraviolet Spectroscopy*; Wiley: New York, 1962; Chapter 17.

(6) Dainese, D. Graduation Thesis, Department of Chemistry, University of Modena, Italy, 1986.

(7) Montaudo, G.; Finocchiaro, P.; Trivellone, E.; Bottino, F.; Maravigna, P. *J. Mol. Struct.* **1973**, *16*, 299.

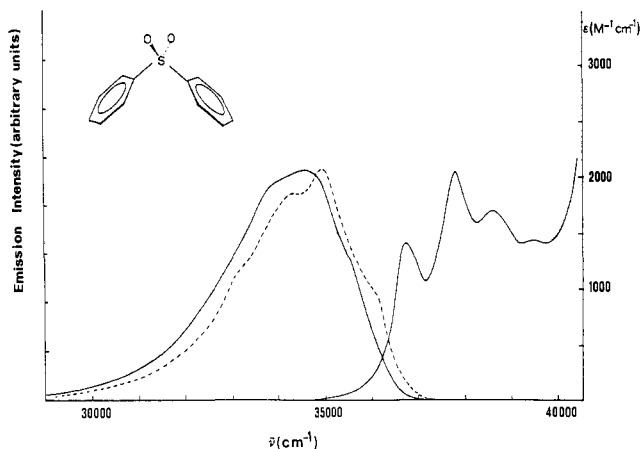


Figure 1. Lowest energy absorption band of DPS in ethanol and corrected fluorescence emission spectra in cyclohexane (---) and ethanol (—). Molar extinction coefficients are taken from ref 4.

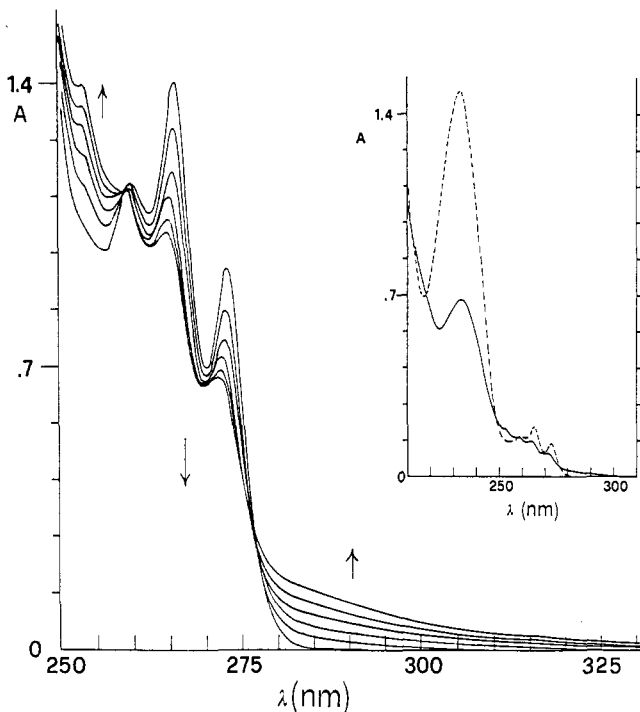


Figure 2. Time evolution of the absorption spectrum (330–250 nm) of DPS in ethanol irradiated with a low-pressure mercury lamp. The arrows indicate the directions of the absorption changes in time. More extended spectra measured before (—) and after (---) irradiation (2 h) are shown in the inset.

> 277 nm in Figure 2. Details on the analytical procedure are given in the Experimental Section.

These observations confirm the conclusions of previous steady-state studies:^{2,8,9} the primary step in the photochemistry of DPS is a C–S homolysis with formation of a phenyl–benzenesulfonyl radical pair. This may undergo cage recombination to give back ground-state DPS or may diffuse apart into the solvent bulk, the fate of the free radicals depending on their properties and on the solvent. In alcohols, the phenyl radicals either will react with the solvent, yielding benzene, phenol, and 1-phenylethanol, or will attack a phenyl ring of DPS to produce 4-biphenyl phenyl sulfone with a mechanism that may be similar to that leading to biphenyl production in the photolysis of DPS in benzene.⁹ The behavior of benzenesulfonyl radicals appears to be more complex. The observed mixed kinetics of the ben-

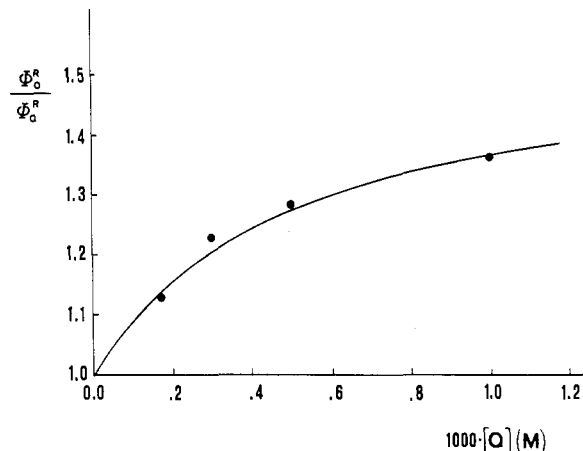


Figure 3. Stern–Volmer plot for the photolysis of DPS in methanol. Diacetyl is the triplet quencher (Q). Φ_0^R and Φ_Q^R are the overall product formation quantum yields in the absence and presence of diacetyl, respectively. The solid curve represents the best fit of eq 10 (Appendix 1) to the experimental points: $\Phi_{S_1}^0/\Phi_{T_1}^0 = 2$, $k_Q\tau_{T_1} = 3 \times 10^3 \text{ M}^{-1}$ (see Appendix 1 and the Experimental Section for more details).

zenesulfonyl radical absorption decay in alcohols¹ suggests that these radicals partition between a second-order disproportionation, leading to benzenesulfonic acid and diphenyl disulfide¹⁰ (but Ph–SO₂–S–Ph is another reasonable disproportionation product), and a first-order or pseudo-first-order process. The latter is likely to reflect the competition between hydrogen abstraction from the alcohol, leading to benzenesulfonic acid, and loss of sulfur dioxide, providing additional phenyl radicals. Our inability to obtain clear spectral evidence for the formation of benzenesulfonic acid may suggest that the second decay route prevails over the first one in ethanol, a conclusion which can also be inferred from the relatively low yield of benzenesulfonic acid production in the photolysis of phenyl benzyl sulfone in as good a hydrogen-donor solvent as 2-propanol.¹¹

In order to see whether or not the S₁ state of DPS contributes to the initial C–S bond cleavage, we measured the rates of growth of the sample absorbance at 295 nm in the absence and presence of diacetyl, whose concentrations were chosen so as to attain a progressive quenching of the lowest triplet state of DPS without significant S₁ quenching (diffusional quenching rate constants were assumed). The absorbance increase at 295 nm is mainly attributed to the formation of 4-biphenyl phenyl sulfone, with smaller contributions arising from Ph–SO₂–S–Ph and Ph–S–S–Ph, and the rate of such increase is proportional to the sums of the quantum yields of formation of these products. After normalization with respect to the photon flux from the mercury lamp, the ratios of the rates measured in the absence and presence of diacetyl reproduced the ratios of the sums of the photoproduct formation quantum yields Φ_0^R/Φ_Q^R (see Appendix 1) and could be plotted versus the quencher concentration, yielding the Stern–Volmer plot of Figure 3. As can be seen, the plot is far from linear but tends rather to an asymptotic value with increasing quencher concentration. From this, we deduce that the photoreaction proceeds from both the S₁ and the T₁ states of DPS.¹² An iterative best fitting of the experimental points to the function $\Phi_0^R/\Phi_Q^R(Q)$ was performed under the simplifying assumption that the absorbance increase at 295 nm was only due to 4-biphenyl phenyl sulfone (see Appendix 1). The best fitting curve is shown in Figure 3 and corresponds to a singlet to triplet reaction quantum yield ratio $\Phi_{S_1}^R/\Phi_{T_1}^R \approx 2$.

(10) Badr, M. Z. A.; Aly, M. M.; Fahmy, A. M. *J. Org. Chem.* **1981**, *46*, 4784.

(11) Langler, R. F.; Marini, Z. A.; Pincock, J. A. *Can. J. Chem.* **1978**, *56*, 903.

(12) Such a result had already been suggested by laser flash photolysis experiments.¹ In that case, however, the fast growth of the absorption probably due to the benzenesulfonyl radical could not be attributed with certainty to its being produced directly from the S₁ state, because of some overlapping T_n ← T₁ absorption.

(8) Kharasch, N.; Khodair, A. I. A. *J. Chem. Soc., Chem. Commun.* **1967**, 98.

(9) Nakai, M.; Furukawa, N.; Oae, S.; Nakabayashi, T. *Bull. Chem. Soc. Jpn.* **1972**, *45*, 1117.

TABLE I: Fluorescence Parameters (Quantum Yields, Φ_{FM} , and Lifetimes, τ_M), Intersystem Crossing Quantum Yields (Φ_{TM}), and Radiative (k_{FM}) and Intersystem Crossing (k_{TM}) Rate Constants at 20 °C^f

	EtOH	MeOH	<i>t</i> -ButOH	C ₆ H ₁₂	CH ₃ CN
Φ_{FM}	0.04	0.04	0.06	0.10	0.05
τ_M , ns	2.8	2.9	4.2	7.8	3.8
Φ_{TM}	0.23 ^a	0.26 ^b	0.27 ^c	0.35 ^a	0.25 ^a
Φ_X^d	0.73	0.70	0.67	0.56	0.70
$k_{FM} \times 10^{-7}$, s	1.4	1.4	1.4	1.3	1.3
$k_{TM} \times 10^{-7}$, s	8.2	9.0	6.4	4.4	6.6
$k_X \times 10^{-7}$, s	26.1	24.1	16.0	7.2	18.4

^a Obtained by dividing by 2 the slopes of the Wilkinson plots (linear least-squares fitting gave the following slopes: 0.46 ± 0.07 in ethanol, 0.70 ± 0.06 in cyclohexane, and 0.50 ± 0.04 in acetonitrile).

^b Measured with the method based on diacetyl phosphorescence sensitization. Uncertainties: $\pm 10\%$. The value in cyclohexane is the average of two values: 0.30 ± 0.03 (reference biphenyl) and 0.36 ± 0.04 (reference phenanthrene). ^c Obtained from relative actinometry and the assumption $(\epsilon_{440}^{T-T})_{EtOH} = (\epsilon_{440}^{T-T})_{BuOH}$. Uncertainty: $\pm 20\%$. ^d $\Phi_X = 1 - \Phi_{FM} - \Phi_{TM}$. ^e $k_X = \Phi_X / \tau_M$. ^f Uncertainties were $\pm 20\%$ on fluorescence quantum yield values and $\pm 10\%$ on lifetimes.

3. Room-Temperature Decay Kinetics of S_1 . With the aim of characterizing the S_1 decay channel which leads efficiently (and independently from the T_1 state) to the C–S homolysis, we analyzed in detail the S_1 deactivation by measuring the fluorescence and $S_1 \rightsquigarrow T_1$ intersystem crossing quantum yields and the fluorescence lifetimes of DPS in ethanol and some other solvents at room temperature. The experimental results are reported in Table I, together with the corresponding calculated rate constants.

We can immediately observe that fluorescence emission plays a minor role in the overall S_1 decay in all solvents employed. Although its quantum yield and lifetime change with the solvent, its calculated radiative rate constants are essentially solvent-independent, a result in keeping with the observed weak or negligible solvent effects on the intensity of the lowest energy absorption band.

A more important role in the S_1 decay is played by $S_1 \rightsquigarrow T_1$ intersystem crossing. Its quantum yields were measured with three different procedures (see the Experimental Section for details). The agreement between values obtained with different methods is good, as can be seen by comparing the two results in cyclohexane and those obtained in ethanol and methanol (Table I). The k_{TM} values exhibit some solvent dependence. They increase from 4.4×10^7 s⁻¹ in cyclohexane, to $(6.4\text{--}6.6) \times 10^7$ s⁻¹ in *tert*-butyl alcohol and acetonitrile, to $(8.2\text{--}9.0) \times 10^7$ s⁻¹ in ethanol and methanol. Thus, both solvent polarity and proticity seem to moderately favor the DPS $S_1 \rightsquigarrow T_1$ intersystem crossing. Any closer investigation of this solvent effect is presently beyond our scope.

Some additional decay pathways must now be considered in order to fulfill the basic condition that the sum of the quantum yields of all the processes that contribute to the S_1 deactivation be equal to one. Their overall quantum yields and rate constants are reported in Table I as Φ_X and k_X . It is evident that these processes are very efficient, actually the dominant ones, in all solvents. As we shall see, a basis for the identification of these processes will be provided both by examination of the temperature dependence of the S_1 decay rate (next paragraph) and by analysis of the kinetic assumptions implicit in our treatment of the Φ_{TM} data obtained with the Wilkinson method (see section 5 and Appendix 2). However, it may be interesting to observe here that k_X exhibits a solvent dependence similar to that of k_{TM} , its value increasing from cyclohexane, to *tert*-butyl alcohol and acetonitrile, to ethanol and methanol in two comparable steps, just as occurs with k_{TM} . This might be taken as a hint that the two processes are alike, i.e., that they are both intersystem crossings, even though caution is certainly necessary in such a difficult subject as the effect of solvent properties on radiationless transition probabilities.

4. Temperature Dependence of τ_M and Nature of the Main S_1 Decay Channel. The fluorescence decay rate constants of DPS

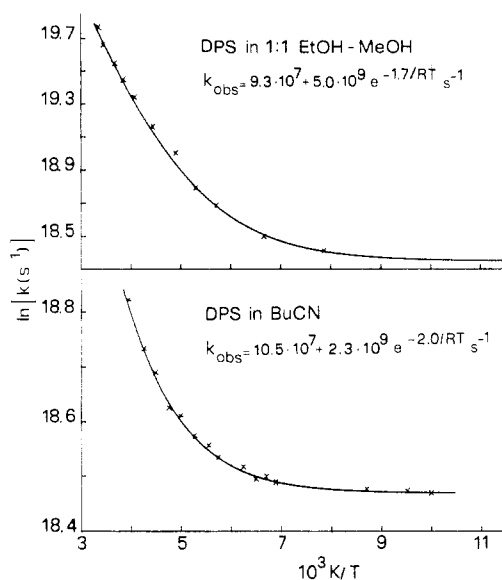


Figure 4. Arrhenius plots of the fluorescence decay constants of DPS in an ethanol–methanol mixture, 1:1 by volume (upper curve), and butyronitrile (lower curve).

in butyronitrile and in a 1:1 ethanol–methanol mixture were measured as functions of temperature in the range 100–298 K. The results are reported in Figure 4. Each of the measured rate constants can be expressed as the sum of a temperature-independent term (k_0) and an activated contribution. An iterative best fitting procedure gave the k_0 values and Arrhenius parameters reported in Figure 4. Both preexponential factors (5×10^9 s⁻¹ in 1:1 ethanol–methanol, 2.3×10^9 s⁻¹ in butyronitrile) are in the range of values expected for a spin-forbidden process, such as an $S_1 \rightsquigarrow T_n$ intersystem crossing.¹³ The nonactivated contribution measured in the alcoholic mixture (9.3×10^7 s⁻¹) compares very closely with the sum of the radiative and $S_1 \rightsquigarrow T_1$ intersystem crossing rate constants (9.6×10^7 s⁻¹ in ethanol, 10.4×10^7 s⁻¹ in methanol) as reported in Table I. As a consequence, the k_X values in ethanol and methanol (26.1×10^7 and 24.1×10^7 s⁻¹, respectively) coincide, within the experimental errors, with the value of the activated term of k_{obs} in the alcoholic mixture at 293 K (26.7×10^7 s⁻¹). This coincidence of independently obtained rate data, together with the mentioned behavior of k_X with solvent, strongly suggests that the unknown additional X process is an $S_1 \rightsquigarrow T_n$ intersystem crossing, characterized by an activation energy of about 2 kcal/mol. Further support for this hypothesis comes from its ability to explain the important role played by the S_1 state, independently of T_1 , in the photolysis of DPS in alcohols.

5. Extension to S_1 of the Photodissociation Model. The observations concerning the S_1 decay of DPS in alcohols that we have described so far (important direct contribution to photodissociation, activated $S_1 \rightsquigarrow T_n$ intersystem crossing as the major deactivation pathway) find a rationalization in the model potential energy diagram depicted in Figure 5. This model is a simple extension, including the S_1 potential energy curve, of the one already proposed to describe the triplet mechanism of the DPS photodissociation.¹ Figure 5 reports the potential energies of the ground state and three relevant excited states as functions of the dissociation coordinate. S_1 and $T_1(\pi\pi^*)$ are the lowest excited singlet and triplet states involving the π electrons of the phenyl rings, while $^3\sigma\sigma^*$ indicates a higher energy triplet involving the bonding and antibonding orbitals of a C–S bond. The dashed lines represent the crossing between the $^3\sigma\sigma^*$ repulsive curve and the $^3\pi\pi^*$ curve, a crossing which occurs in a zeroth-order description and becomes avoided (solid lines) as soon as σ – π interactions are allowed for.¹ Such a crossing avoidance will occur between the S_1 and $^3\sigma\sigma^*$ curves on the sole condition that appreciable spin–orbit coupling be operative.

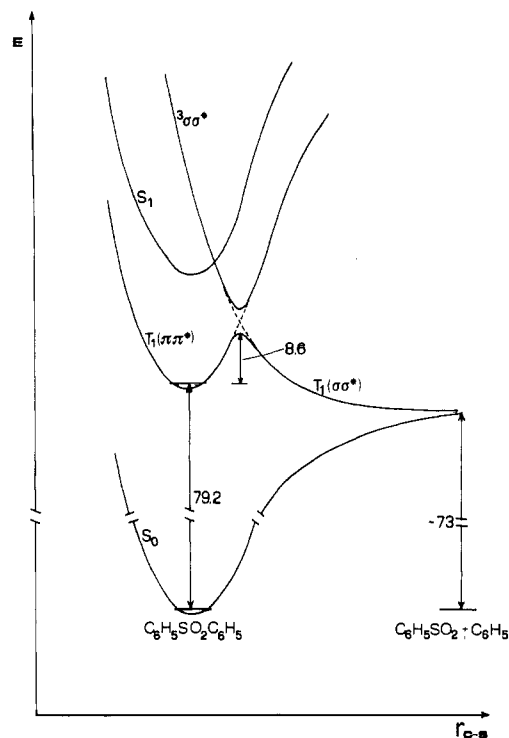


Figure 5. Model potential energy curves of the ground state and three relevant excited states of DPS along the stretching coordinate of a C-S bond (see text for a detailed description). Energies are given in kcal/mol and are taken from ref 1.

The working hypothesis emerging from Figure 5 is that passage from the spectroscopic minima of S_1 and T_1 to the dissociative triplet *adiabatic*¹ curve provides a reactive pathway for both states. In a localized representation, each such passage may be viewed as a "migration" of electronic excitation from the aromatic moieties ($\pi\pi^*$ excitation) to the stretched C-S bond ($\sigma\sigma^*$ excitation). Finally, some of the excitation energy may be converted into translational energy of the molecular fragments, i.e., of the phenyl and benzenesulfonyl radicals in their doublet ground states. Alternatively, the radical pair formed on the triplet dissociative curve may undergo a spin flip and subsequent cage recombination to give back ground-state DPS. This, however, is usually considered an unlikely process.¹⁴ The energy barriers which hinder the passage from S_1 and $T_1(\pi\pi^*)$ to the $^3\sigma\sigma^*$ curve have different natures. The barrier opposing the reactive decay of T_1 is just a feature of one and the same Born-Oppenheimer *adiabatic*¹ surface, so that Arrhenius preexponential factors in the range 10^{12} – 10^{14} s⁻¹ are expected, and actually observed,¹ for this process. On the contrary, according to the model of Figure 5, the reactive pathway of S_1 is an activated intersystem crossing. Thus, an activation energy roughly corresponding to the energy of the $S_1 \rightarrow ^3\sigma\sigma^*$ crossing point relative to the spectroscopic S_1 minimum is expected to characterize the reactive decay of S_1 , together with a preexponential factor lower than 10^{12} s⁻¹ (typical values for polyacenes are 10^8 – 10^9 s⁻¹).¹³ Our kinetic measurements in 1:1 ethanol-methanol and butyronitrile ($E_a = 1.7$ – 2.0 kcal/mol, $A = (2.3$ – $5.0) \times 10^9$ s⁻¹) are thus qualitatively accounted for by the model diagram of Figure 5.

A more careful analysis of the $S_1 \rightarrow T_n$ intersystem crossing probabilities, in light of spin-orbit coupling theory¹⁵ provides a more detailed interpretation of the $S_1 \rightarrow ^3\sigma\sigma^*$ intersystem crossing, thus suggesting a slightly modified reading of the model diagram of Figure 5. Due to the mono-electronic nature of the spin-orbit coupling Hamiltonian,¹⁵ a matrix element such as $\langle ^1\pi\pi^* | H_{so} | ^3\sigma\sigma^* \rangle$ is zero. As a consequence, a direct $S_1(\pi\pi^*) \rightarrow$

$^3\sigma\sigma^*$ intersystem crossing is forbidden at this description level. However, the S_1 and $^3\sigma\sigma^*$ states of Figure 5 are described by multiconfigurational wave functions, as shown by the mentioned CS-INDO/CI calculation.⁶ Actually, the wave functions of the two almost degenerate 1L_b states contain significant contributions from a few monoexcited configurations, some of which have nonvanishing spin-orbit coupling with the almost monoconfigurational $^3\sigma\sigma^*$ state. Furthermore, analysis of the calculated wave functions shows that several other triplet states, whose energies are calculated close to the energies of the 1L_b states at the S_0 equilibrium geometry, have nonzero spin-orbit coupling terms with the 1L_b states. Thus, these triplet states might contribute to the overall $S_1 \rightarrow ^3\sigma\sigma^*$ intersystem crossing by acting as bridging states, which would efficiently convert to the $^3\sigma\sigma^*$ dissociative state. Such an hypothesis on the $S_1 \rightarrow ^3\sigma\sigma^*$ intersystem crossing is by no means alternative to the one based on a direct passage. Both a direct and some indirect $S_1 \rightarrow ^3\sigma\sigma^*$ intersystem crossings probably occur. As a consequence, the measured Arrhenius parameters for the S_1 decay probably represent mean values of more than one activated intersystem crossing, as appears to be often the case with room-temperature $S_1 \rightarrow T_n$ intersystem crossing.¹³ This is the meaning that we assign to the model diagram of Figure 5: $S_1 \rightarrow ^3\sigma\sigma^*$ intersystem crossing is probably an overall process to which several activated processes contribute.

Strong support for the correctness of the model diagram of Figure 5 comes from the good agreement between the Φ_{TM} values measured in cyclohexane and methanol with the method based on diacetyl phosphorescence sensitization and the values obtained in cyclohexane and ethanol dividing by 2 the measured slopes of the Wilkinson plots (Table I). In fact, the latter data treatment results from the working-out of a kinetic scheme based on the model diagram of Figure 5 (see Appendix 2). Thus, the observed agreement between the two sets of Φ_{TM} values provides indirect support for the proposed model.

Conclusions

The results of our investigation of the S_1 decay mechanisms of DPS in alcohols are found to design a complete and self-consistent scheme. A rationalization of these results is achieved through a simple extension to S_1 of a model potential energy diagram that proved able to account for the observed decay kinetics of the T_1 state. The dominant S_1 decay path is suggested to be an activated intersystem crossing leading to population of a C-S dissociative triplet state and, eventually, to the homolytic cleavage of a C-S bond.

The reactive decay of the DPS S_1 state appears to slow down on changing the solvent from ethanol and methanol to acetonitrile to cyclohexane, to the advantage of fluorescence and $S_1 \rightarrow T_1$ intersystem crossing quantum yields.

Our proposal parallels the early suggestion of Land and Porter¹⁶ which explained the S_1 role in the OH homolysis of phenol in terms of an intersystem crossing to a dissociative triplet state localized on the OH bond.

Experimental Section

Materials. DPS was synthesized according to the procedure of ref 17 and recrystallized twice in ethanol. Ethanol (95% Carlo Erba RPE-ACS) and methanol (Merck, p.a.) were distilled from CaCl₂; the central fractions were collected and kept under nitrogen atmosphere. Butyronitrile (Merck, for synthesis) was distilled, and the central fractions were collected. Acetonitrile (Merck, p.a.) was refluxed over P₂O₅ and distilled, and the central fractions were collected over MgSO₄. *tert*-Butyl alcohol (Merck, p.a.) was refluxed over sodium and distilled. Cyclohexane (Merck, for fluorescence spectroscopy) was used without further purification. Diacetyl (Fluka, puriss.) was distilled under vacuum at room temperature and utilized shortly after.

Steady-State Photolysis and Product Analysis. DPS was irradiated in alcohols with a low-pressure mercury arc lamp.

(14) Koenig, T.; Fischer, H. In *Free Radicals*; Kochi, J. K., Ed.; Wiley: New York, 1973; Vol. 1, Chapter 4.

(15) McGlynn, S. P.; Azumi, T.; Kinoshita, M. *Molecular Spectroscopy of the Triplet State*; Prentice-Hall: Englewood Cliffs, NJ, 1969; Chapters 5 and 6.

(16) Land, E. J.; Porter, G. *Trans. Faraday Soc.* **1963**, *59*, 2016.

(17) Knüßli, E. *Gazz. Chim. Ital.* **1949**, *621*; **1950**, *522*.

Solutions were deaerated by standard methods and were gently stirred during irradiation. Analysis of the photolysis products was mainly based on their UV absorption and fluorescence spectra. The formation of benzene was established on the basis of the appearance of its structured absorption between 240 and 260 nm in the spectrum of the photolyzed solution and was confirmed by GC analysis. Benzenesulfonic acid was identified by comparison of the literature UV absorption of its anion¹⁸ with the spectrum of the alkaline aqueous solution of the photoproducts. The presence in this solution of 1-phenylethyl alcohol and phenol was suspected on the basis of its fluorescence and absorption spectra and on their dependence on pH¹⁸⁻²⁰ and on the slightly positive result of the FeCl₃ test for phenols.²¹ The water-insoluble photoproducts were treated with *n*-hexane, and the solution was chromatographed in an Al₂O₃ column with a 1:1 *n*-hexane-dioxane mixture as the eluent. Ph-SO₂-S-Ph and 4-biphenyl phenyl sulfone were separated and identified from their absorption spectra.^{22,23} Finally, we attribute the extremely long tail of the absorption spectra of the photolyzed solution to the formation of diphenyl disulfide.²⁴

Quantitative information on the effect of diacetyl on the photoproduct formation quantum yields was obtained by measuring the rate of the absorbance increase at 295 nm with the irradiation time. Since three products (4-biphenyl phenyl sulfone, Ph-SO₂-S-Ph, and Ph-S-S-Ph) are at least responsible for this rising absorption, some care is required in the data analysis (see Appendix 1). The slopes of the A_{295}/t plots were calculated at the origin, in order to minimize the nonlinearity effects due to the increasing absorption of the photolysis products at the irradiation wavelength. The slopes so obtained were normalized relative to the incident photon flux I determined by ferrioxalate actinometry.²⁵ All samples had the same DPS absorbance at 253.7 nm. Diacetyl absorbance at this wavelength was always negligible. In order to apply the simplified expression of the slope ratios derived in Appendix 1 (eq 10), the assumption was made that A_{295} was due to only one product, 4-biphenyl phenyl sulfone, the other contributions being considered negligible. The experimental points were fitted to the simplified equation, $\Phi_{S_1}^0/\Phi_{T_1}^0$ and k_{QT} being varied in the iterative best fitting procedure.

Fluorescence Spectra, Quantum Yields, and Lifetimes. The fluorescence spectra were measured on a Jobin-Yvon JY 3CS spectrofluorometer and corrected for the instrumental response curve. Fluorescence quantum yields were determined relative to *p*-cresol in cyclohexane ($\Phi_{FM} = 0.09$ ¹⁹). The commonly applied correction ($1/n^2$) due to the refractive index variation was introduced for the determinations in other solvents.²⁶ Sodium D-line refractive indexes were used. Fluorescence lifetimes were measured with an SP70 Applied Photophysics single-photon counting equipment interfaced to a HP 85 personal computer. All samples were deaerated, either by thorough nitrogen bubbling or by four freeze-pump-thaw cycles. Deconvolution of the decay profiles from the exciting pulse was performed by the standard phase-plane method.²⁷ Decays were monoexponential. Temperature variation in the range 80–300 K was achieved by means of a modified Thor nitrogen flow cryostat (Model C610).

$S_1 \rightsquigarrow T_1$ Intersystem Crossing Yields. Three different methods were used for the determination of DPS $S_1 \rightsquigarrow T_1$ intersystem crossing yields. The first one was based on the diacetyl

phosphorescence sensitization by the DPS T_1 state and was employed in cyclohexane and methanol. We followed the procedure given in ref 28. Phenanthrene was used as the reference donor in methanol; biphenyl and phenanthrene were used in cyclohexane. The sample (DPS) and reference solutions were all irradiated at 270 nm. OD's were such that all the incident light was absorbed. Absorption by diacetyl was always negligible. All the samples were degassed by three freeze-pump-thaw cycles. The total emission spectra (donor fluorescence plus diacetyl sensitized phosphorescence) were corrected. Diacetyl concentration was varied so as to ensure complete triplet quenching of all the donors (but negligible singlet quenching). The following values were used for Φ_{TM} and Φ_{FM} of the reference compounds: for phenanthrene $\Phi_{TM} = 0.825$ and $\Phi_{FM} = 0.13$ ²⁹ in methanol, $\Phi_{TM} = 0.79$ ^{28,29} and $\Phi_{FM} = 0.15$ ^{19,28,29} in cyclohexane; for biphenyl in cyclohexane, $\Phi_{TM} = 0.81$ ²⁹ and $\Phi_{FM} = 0.18$.¹⁹

The $S_1 \rightsquigarrow T_1$ quantum yield in *tert*-butyl alcohol was measured with a method based on relative actinometry.³⁰ The DPS $T_n \leftarrow T_1$ absorption was measured at 440 nm with an excimer laser flash photolysis apparatus described elsewhere.³¹ DPS in ethanol was used as the reference solution. The assumption was made that ϵ_{440}^T was the same in *tert*-butyl alcohol and in ethanol. The value in the latter solvent ($\epsilon_{440}^T = 9200 \text{ M}^{-1} \text{ cm}^{-1}$) was measured relative to naphthalene in cyclohexane ($\Phi_{TM} = 0.75$,³⁰ $\epsilon_{415}^T = 24500 \text{ M}^{-1} \text{ cm}^{-1}$ ³²) by using the Φ_{TM} value obtained with the method described next. Effects due to the exciting pulse energy were always taken into account in the data analysis.

The $S_1 \rightsquigarrow T_1$ quantum yields of DPS in ethanol, cyclohexane, and acetonitrile were measured with a method based on the effect on intersystem crossing rates of an external heavy atom, such as xenon.³³ Fluorescence emission intensities and $T_n \leftarrow T_1$ absorption intensities were measured at variable xenon concentration, and the results were combined in a plot whose slope coincides with Φ_{TM} in the original Wilkinson kinetic analysis. As is shown in section 5 and Appendix 2, the kinetic model that applies to the DPS S_1 state decay is different from the one used by Wilkinson for many aromatic hydrocarbons. The DPS plots are still expected to be linear, but their slopes should be about twice the value of Φ_{TM} . Indeed, linear plots were obtained in all the solvents employed.

Acknowledgment. Prof. F. Momicchioli is warmly thanked for his many useful suggestions and for his careful revision of the original manuscript. Mr. M. Bandiera's technical assistance is gratefully acknowledged. Prof. I. Baraldi is thanked for making available to us his preliminary theoretical data on DPS, partly reported in ref. 6. Prof. D. Iarossi is thanked for supplying DPS. M.S. thanks Prof. C. Bartocci and Dr. A. Maldotti of the University of Ferrara for their support in the steady-state photolysis measurements. This work was financially supported by the Ministero della Pubblica Istruzione (Roma).

Appendix 1

Effect of a Triplet Quencher on the Rate of Absorbance Increase. If a number of photolysis products absorb at some monitoring wavelength λ , at which reagents do not absorb, the measured absorbance can be expressed as

$$A^\lambda(t) = \bar{\epsilon}^\lambda c_{\text{tot}}(t) \quad (1)$$

where

$$\bar{\epsilon}^\lambda = c_{\text{tot}}^{-1} \sum_i \epsilon_i^\lambda c_i \quad (2)$$

ϵ_i^λ being the extinction coefficient of the *i*th product, which is present at concentration c_i , and

(18) *UV Atlas of Organic Compounds*; Verlag-Chemie: Weinheim, 1966; Vol. 2.

(19) Berlman, I. B. *Handbook of Fluorescence Spectra of Aromatic Molecules*; Academic: New York, 1971.

(20) Truong, T. B.; Petit, A. *J. Phys. Chem.* **1979**, *83*, 1300.

(21) Wesp, E. F.; Brode, W. R. *J. Am. Chem. Soc.* **1934**, *56*, 1037.

(22) Mangini, A. *Gazz. Chim. Ital.* **1958**, *88*, 1063.

(23) Mangini, A.; Ruzzier, L.; Tundo, A. *Boll. Sci. Fac. Chim. Ind. Bologna* **1956**, *14*, 81.

(24) *Absorption Spectra in the Ultraviolet and Visible Region*; Lang, L., Ed.; Hungarian Academy of Sciences: Budapest, 1961; Vol. XV.

(25) Murov, S. L. *Handbook of Photochemistry*; Marcel Dekker: New York, 1973.

(26) Demas, J. N.; Crosby, G. A. *J. Phys. Chem.* **1971**, *75*, 991.

(27) Greer, J. M.; Reed, F. W.; Demas, J. N. *Anal. Chem.* **1981**, *53*, 710.

(28) Bonnier, J.-M.; Jardon, P. *J. Chim. Phys.* **1970**, *67*, 577.

(29) Wilkinson, F. In *Organic Molecular Photophysics*; Birks, J. B., Ed.; Wiley: London, 1975; Vol. 2, Chapter 3.

(30) Amand, B.; Bensasson, R. *Chem. Phys. Lett.* **1975**, *34*, 44.

(31) Longoni, A.; Ponterini, G. *Appl. Spectrosc.* **1986**, *40*, 599.

(32) Bensasson, R.; Land, E. J. *Trans. Faraday Soc.* **1971**, *67*, 1904.

(33) Horrocks, A. R.; Kearvell, A.; Tickle, K.; Wilkinson, F. *Trans. Faraday Soc.* **1966**, *62*, 3393.

$$c_{\text{tot}} = \sum_i c_i \quad (3)$$

$\bar{\epsilon}^\lambda$ is time-independent if the products are formed in constant proportions. We define the i th product formation quantum yield

$$\Phi_i = \frac{c_i(t)}{I t} \quad (4)$$

where t is the irradiation time and I is the number of moles of photons absorbed per liter of solution per second and is considered constant. Substitution of (3) and (4) in (1) yields

$$A^\lambda(t) = \bar{\epsilon}^\lambda I \sum_i \Phi_i t \quad (5)$$

Thus, the slope of an $A^\lambda(t)/t$ plot, as long as this is linear, equals $\bar{\epsilon}^\lambda I \sum_i \Phi_i$. After normalization with respect to the incident photon flux I , the ratios of the slopes in the absence and presence of a quencher Q can be written as

$$m_0/m_Q = \sum_i \Phi_i^0 / \sum_i \Phi_i^Q = \Phi_0^R / \Phi_Q^R \quad (6)$$

where Φ_0^R and Φ_Q^R are the total photoproduct formation quantum yields in the absence and presence of quencher, respectively. If we limit the quencher concentrations so as to quench only the T_1 state of the reagent and express the effect of triplet quenching by the usual Stern-Volmer expression

$$\Phi_{T_1}^0 / \Phi_{T_1}^Q = 1 + k_Q \tau_{T_1} [Q] \quad (7)$$

where k_Q is the T_1 quenching rate constant and τ_{T_1} is the triplet lifetime in the absence of quencher, we finally obtain

$$m_0/m_Q = \Phi_0^R / \Phi_Q^R = \frac{\sum_i \Phi_i^0}{\sum_i (\Phi_i^0 + \Phi_{S_1}^0 k_Q \tau_{T_1} [Q])} (1 + k_Q \tau_{T_1} [Q]) \quad (8)$$

A linear Stern-Volmer plot is thus obtained only if $\Phi_{S_1}^0$, the S_1 contributions to photoproduct formation, are negligible. A simplification of eq 8 can be obtained and used for a best fitting procedure of the experimental points of a nonlinear Stern-Volmer plot, if we assume that most of the absorbance A^λ is due to only one product. In this case, eq 8 becomes

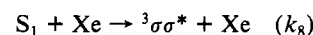
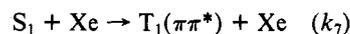
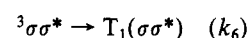
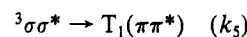
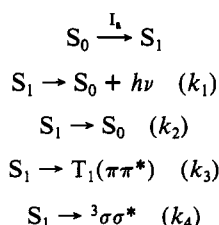
$$m_0/m_Q = \Phi^0 (1 + k_Q \tau_{T_1} [Q]) / (\Phi^0 + \Phi_{S_1}^0 k_Q \tau_{T_1} [Q]) \quad (9)$$

which can be expressed in terms of two fitting parameters, $k_Q \tau_{T_1}$ and $\Phi_{S_1}^0 / \Phi_{T_1}^0$, as follows:

$$m_0/m_Q = \frac{\Phi_{S_1}^0 / \Phi_{T_1}^0 + 1}{\Phi_{S_1}^0 / \Phi_{T_1}^0 + 1 + \Phi_{S_1}^0 k_Q \tau_{T_1} [Q] / \Phi_{T_1}^0} (1 + k_Q \tau_{T_1} [Q]) \quad (10)$$

Appendix 2

Effect of Xenon on the Triplet Quantum Yield of DPS. With reference to the model diagram of Figure 5, let us consider all the processes that affect the fluorescence and $T_n \leftarrow T_1$ absorption intensity measurements necessary for the determination of the $S_1 \rightsquigarrow T_1$ intersystem crossing quantum yield with the Wilkinson method:³³



If F^0 and F are the fluorescence intensities at some monitoring wavelength in the absence and presence of xenon, respectively, and if $F^0/F = \Phi_{FM}^0/\Phi_{FM}$, then

$$F^0/F = 1 + (k_7 + k_8)\tau_M[\text{Xe}] \quad (11)$$

where τ_M is the fluorescence lifetime in xenon-free solutions. The $S_1 \rightsquigarrow T_1$ intersystem crossing quantum yield Φ_{TM} can be expressed as

$$\Phi_{TM} = \Phi_{S_1 \rightsquigarrow T_1(\pi\pi^*)} + \Phi_{S_1 \rightsquigarrow {}^3\sigma\sigma^*} \phi_{\sigma\sigma^*} \rightarrow T_1(\pi\pi^*) \quad (12)$$

where Φ and ϕ denote quantum yields and efficiencies, respectively.

Expression of the right-hand terms of eq 12 in the absence (Φ_{TM}^0) and presence (Φ_{TM}) of xenon is straightforward, and the corresponding ratio of the observed $T_n \leftarrow T_1$ absorption intensities can be written as

$$\text{OD}_T / \text{OD}_T^0 = \Phi_{TM} / \Phi_{TM}^0 = \frac{k_3(k_5 + k_6) + k_4k_5 + [k_7(k_5 + k_6) + k_5k_8][\text{Xe}]}{[k_3(k_5 + k_6) + k_4k_5][1 + (k_7 + k_8)\tau_M[\text{Xe}]]} \quad (13)$$

Combining eq 11 and 13 and making the substitution $[\text{Xe}] = 1/[(k_7 + k_8)\tau_M(F^0/F - 1)]$, one finally obtains for the Wilkinson plot ($F^0/F - 1$) versus $(\text{OD}_T F^0 / \text{OD}_T^0 F - 1)$

$$F^0/F - 1 = (\text{OD}_T F^0 / \text{OD}_T^0 F - 1) \left(1 + \frac{k_6 k_8}{k_5(k_7 + k_8) + k_6 k_7} \right) \Phi_{TM}^0 \quad (14)$$

Thus, even in this case, where two competitive intersystem crossings can be simultaneously enhanced by the external heavy-atom effect of xenon, the Wilkinson plot is expected to be linear. However, its slope p will no more merely coincide with Φ_{TM}^0 . If we assume k_7 and k_8 to be of the same order of magnitude, then two limiting values can be envisaged for the slope p of this plot: if $k_6 \ll k_5$, then $p \sim \Phi_{TM}^0$; if $k_6 \gg k_5$, then $p \sim 2\Phi_{TM}^0$. The latter case corresponds to a complete conservation of the direction of motion by the molecules that approach the avoided crossing region on the ${}^3\sigma\sigma^*$ state surface, whereas the former one requires a change in the nature (from ${}^3\sigma\sigma^*$ to ${}^3\pi\pi^*$) of the electronic wave function in the passage across the avoided crossing. Also, the internal conversion from the upper to the lower triplets would occur to the vibrational discrete of the bound $T_1(\pi\pi^*)$ state in the former case and to the translational continuum of the two radicals on the dissociative $T_1(\sigma\sigma^*)$ branch in the latter case. So, both the electronic and the state density factors are expected to favor dissociation with respect to population of the bound $T_1(\pi\pi^*)$ state, thus justifying the assumption that $k_6 \gg k_5$ and $p \sim 2\Phi_{TM}^0$. This conclusion is also in keeping with the classical Landau-Zener treatment of surface hopping.³⁴ In fact, both the high slope of the ${}^3\sigma\sigma^*$ dissociative curve and the small energy gap at the avoided crossing (energy gaps of 0.2–0.3 eV were calculated for some ${}^3\sigma\sigma^* \rightarrow {}^3\pi\pi^*$ avoided crossings in chlorobenzene³⁵) should cause the upper left-lower right hopping probability to approach unity.

Registry No. DPS, 127-63-9; Ph-Ph-SO₂-Ph, 1230-51-9; Ph-SO₂-S-Ph, 1212-08-4; Ph-S-S-Ph, 882-33-7; benzene, 71-43-2; benzenesulfonic acid, 98-11-3; diacetyl, 431-03-8.

(34) Salem, L. *Electrons in Chemical Reactions: First Principles*; Wiley: New York, 1982; Chapter 5.

(35) Nagaoka, S.; Takemura, T.; Baba, H.; Koga, N.; Morokuma, K. *J. Phys. Chem.* 1986, 90, 759.